Volume 9, Issue 2, 2020, 1064 - 1073 ISSN 2284-6808

Letters in Applied NanoBioScience

https://nanobioletters.com/

https://doi.org/10.33263/LIANBS92.10641073

Original Research Article Open Access Journal

Received: 01.04.2020 / Revised: 03.05.2020 / Accepted: 06.05.2020 / Published on-line: 10.05.2020

# Chemical, electrochemical and surface morphology investigation of *Cichorium intybus* extract (CIE) as beneficial inhibitor for Al in 2 M HCl acid

**Abd El-Aziz S. Fouda [1, *], Salah M. Rashwan [2], Medhat M. Kamel [2], Eslam Abdel Haleem [1, 3]**

[1] Department of Chemistry, Faculty of Science, El-Mansoura University
[2] Department of Chemistry, Faculty of Science, Suez Canal University
[3] Department of Basic Science, Higher Institute of Engineering and Technology in El-Arish

*corresponding author e-mail address: ***asfouda@hotmail.com*** | Scopus ID 56231506400

## ABSTRACT

The inhibiting activity of CIE(CIE) to the dissolution of Al in 2M HCl medium was carried out by chemical strategies (mass loss and gasometry) and electrochemical systems, for example, tafel polarization (TP), electrochemical impedance spectroscopy (EIS) and electrochemical frequency modulation (EFM). Surface morphology was examined utilizing atomic force microscopy (AFM) and x-ray photoelectron spectroscopy (XPS). Fourier transform infrared spectroscopy (FTIR) outcomes indicated that the inhibition mechanism was by adsorption process through the functional groups that exist in the investigated extract. The results demonstrated that the inhibiting efficiency expanded with expanding amounts of the extract. Polarization information demonstrated that CIE goes about as an inhibitor of mixed type. The procedure of adsorption on Al surface ascribed to Langmuir isotherm. All thermodynamic calculations were determined and discussed. The inhibitive efficiencies obtained from all utilized procedures have acceptable values.

**Keywords:** *CIE(CIE); AFM; FTIR; XPS; Langmuir isotherm.*

## 1. INTRODUCTION

Hydrochloric corrosive mediums are broadly utilized for corrosive pickling, purifying, oil oxidization [1–4]. Al has a surprising monetary, little weight, perfect electric and thermic conductivity. The major significant component in Al is its dissolution opposition because of the development of a defensive form on its outer surface upon its introduction to air or fluid arrangements. Inhibiting of dissolution of Al is a reason for various examinations because of their high mechanical estimation and a wide scope of modern and home hold uses. Utilizing organic particles as dissolution inhibitors might be the principal decision to diminish the dissolution level of metals in corrosive mediums [5-8].

Regardless of the expansive range of organic inhibitors, the decision of proper inhibitor is confined by a few variables. The variables incorporate expanded natural mindfulness and the need to advance earth inviting procedure. Numerous past investigations demonstrated that the natural particles of plant are effective environmentally inhibitors for dissolution [9-11]. The normal results of plant extract are cheap, eco-friendly dissolution inhibitors. The extracts from their roots and leaves illustrated a blend of natural product particles that been accounted for as powerful inhibitors for the dissolution of different metals [12-19].

This research was prepared to discuss the inhibitive influence of Al dissolution in 2M HCl medium in nearness of various amounts of CIEand to consider the impact of temperature on its effectiveness. Likewise to examine the outer surface of aluminum samples without and with Cichorium Intybus extract.

## 2. MATERIALS AND METHODS

### 2.1. Solutions and Materials.

#### *2.1.1. Composition of tested samples.*

Al specimens utilized in this investigation were taken from Al with purity of 99.99 %.The dimensions of these samples 2 x 2 x 0.5 cm.

#### *2.1.2. Corrosive medium.*

The destructive solution (2M HCl) was set by diluting with bi-distilled water from the corrosive medium (34%). The standard solution of $Na_2CO_3$ was utilized to check the prepared concentrations.

#### *2.1.3. Cichorium Intybus extract.*

The extract was acquired utilizing the fine dried powder of Cichorium Intybus leaves, at that point dissolved in $CH_3OH$ and left for seven days. The aqueous medium was purified at 40˚C to eliminate the alcohol from the Cichorium Intybus arrangement and afterward left to dryness. The dried residues were dissolved in 3ml of Di methyl sulfoxide (DMSO) and finished to 1000 ml with ethanol lastly put away under cooling in tightly closed flaskes.

#### *2.1.4. Chemical constituent of Cichorium Intybus extract.*

CIEis full of organic materials such as chalcone, scopoletin, mandelic acid, lupeol and naphthalene [20, 21]. The main components of this extract are shown in Table 1

#### *2.2.1. Chemical Measurements.*

*2.2.1.1. Gasometry.*

$H_2$ development is a beneficial strategy to calculate the measure of $H_2$ creating during the procedure. The container is joined by a flexible part of a burette. From the start, the amount of air was evaluated. At last, aluminum sheets were put in the corrosive medium and the utilized vial was inclosed. The released $H_2$ gas was dictated by the diminishing of the medium grade in the vial at specified times.

*2.2.1.2. Mass Loss.*

The mass tests were achieved utilizing examples of Al with volumes (2x2x0.05cm). The examined Al pieces were weighed up to 4th decimal put utilizing computerized electric adjusts. The analyzed pieces were submerged in 100 mL of 2 M HCl in non-attendance and nearness of shifting amounts of CIE exist at temperatures extend from 25 to 45 $^0$C in water thermostat. Starting weight of tests were measured some time recently submersion after fixed periods of exposure, Al sample was removed from the medium, dried among filter sheets and weighed once more. The change in weight for several times (30-180) minutes was tabled. The tests were achieved at different amounts (50-300 ppm) of CIE. From the average mass loss comes about (normal of three duplicate investigations), the corrosion rate, the level of surface coverage (θ) and the rate of % IE were studied utilizing equation (1):

$$\%IE = \theta \times 100 = [(W^o - W)/W^o] \times 100 \quad (1)$$

Where $W^o$ and W are the estimations of the mass losses in the absence and presence of the inhibitor, separately. The estimations of θ and % IE were illustrated at various amounts of CIE in 2 M HCl.

**Table 1.** The chemical components exist in Cichorium Intybus leaves extract.

| Name | Structure | Molecular Formula |
|---|---|---|
| Scopoletin | 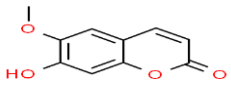 7-Hydroxy-6-methoxy-2H-chromen | $C_{10}H_8O_4$ |
| Mandelic Acid | 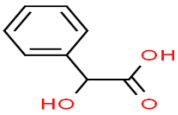 2-Hydroxy-2-phenylethanoic Acid | $C_8H_8O_3$ |
| Lupeol | 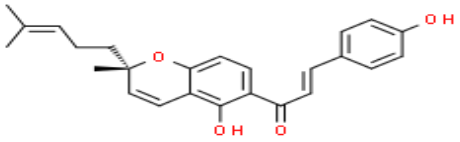 (2E)-1-[(2S)-5-Hydroxy-2-methyl-2-(4-methyl-3-penten-1-yl)-2H-chromen-6-yl]-3-(4-hydroxyphenyl)-2-propen | $C_{25}H_{26}O_4$ |

***2.2.2. Electrochemical Techniques.***

Every electrochemical estimation (TP, EIS and EFM) were completed utilizing Gamry structure framing dependent on ESA400.Gamry usages incorporate programming DC105 for Tafel polarization, EIS300 for EIS tests and EFM140 for EFM tests; PC was utilized for gathering information. Echem Analyst 5.5 Software was utilized for graphing, charting and providing informations. Every utilized estimation completed utilizing a customary cell having 3 cathodes were utilized. The working electrode acts as aluminum sheet (1 $cm^2$) was utilized.

*2.2.2.1. Electrochemical frequency modulation technique.*

The studied system (EFM) is a recent device for observing the electrochemical dissolution. The EFM procedure is recently revealed [22]. EFM has numerous highlights [23-27]. EFM is a non-damaging method, fast check, affords straight forwardly estimation of the dissolution current without earlier knowledge of Tafel parameters and has a perfect quality due to causality values, that illustrate an inner test on the veracity of the EFM estimation.

*2.2.2.2. Tafel polarization method.*

In Tafel polarization estimations, the utilized cell consists of 100 ml of the examined medium. The tafel bends among potential and current were computed by shifting the potential automatically from - 0.8 to 0.5 V at a scan average of 1mV$s^{-1}$. The values of θ and % IE were determined to utilize according to eq. (2):

$$\% IE = \theta \times 100 = [(i_{corr} - i_{corr(inh)}) / i_{corr}] \times 100 \quad (2)$$

Where $i_{corr(inh)}$ and $i_{corr}$ are the corrosion current density values in the existence and non-existence of CIE respectively.

*2.2.2.3. Electrochemical impedance spectroscopy method (EIS).*

The test impedances were completed and clarified dependent on the equivalent circuit. The principal factors found from the assessment of the Nyquist chart are the polarization resistance Rp and the limit of the capacity of double layer Cdl that is described as [28]:

$$C_{dl} = 1/ (2 \pi f_{max} R_P) \quad (3)$$

Where $f_{max}$ is the angular frequency that resulted in its most extreme characteristics. All calculations got from the impedance estimations are described by the next relation:

$$\% IE = [1- (R^{\circ}_P/R_P)] \times 100 \quad (4)$$

Where $R_p$ and $R^o_p$ are the polarization resistance in the existence and non-attendance of CIE, respectively.

$$C_{dl} = 1/ (2 \pi f_{max} R_P)$$

***2.2.3. Surface Morphology.***

*2.2.3.1. Atomic force microscopy (AFM) analysis.*

The favored component of AFM is the roughness of the outer surface of Al samples. The surface deviations caused the observed roughness from its optimal shape. AFM technique was inspected utilizing Nano Surf Easy sweep 2 Flex AFM procedure (Nanotechnology Center, Mansoura University).

*2.2.3.2. Fourier transform infrared examination (FTIR.)*

FTIR spectrum is listed in a Perkin – Elmer 1600 spectrophotometer. The formed layer was closely separated, mixed totally with KBr made into grains and FTIR spectrum is observed.

.

## 3.RESULTS

### 3.1. Gasometry.

The emitted $H_2$ gas coming about because of the dissolution process can be resolved. Results got by the $H_2$ development system in Figure 1 are establishing with various measurements like mass loss and electrochemical procedures. The $H_2$ amount relies on time of response as the next eq. (5):

$$V_{ml} = k_{corr} .t \quad (5)$$

V is the amount of the $H_2$ emitted in mL, t represents time and $k_{corr}$ is corrosion rate at 25C° [29].

The $H_2$ amount was computed every 20 min; $k_{corr}$ and % IE were tabled by eq. (6):

$$\% IE = (1 - k_{corr} / k^{o}_{corr}) \times 100 \quad (6)$$

$k_{corr}$ and $k^{o}_{corr}$ are the corrosion nrates in the presence and non-existence of various doses of CIE, by graphing among ($V_{ml}$ vs. t) and slope is $k_{corr}$.

Table 2 illustrates that the dissolution rate ($k_{corr}$) reduced and inhibitive efficiency (%IE) increased with the rising of CIE concentration.

**Table 2.** IE% and ($k_{corr}$) from HE for the dissolution of Al in 2M HCl without and with several doses of CIEat 25ºC.

| Conc., ppm | $k_{corr}x10^{-3}$, ml/min | %IE |
|---|---|---|
| **Blank** | 1200 | ---- |
| **50** | 275 | 77.1 |
| **100** | 215 | 82.1 |
| **150** | 184.5 | 84.6 |
| **200** | 159.5 | 86.7 |
| **250** | 134 | 88.8 |
| **300** | 125.5 | 89.5 |

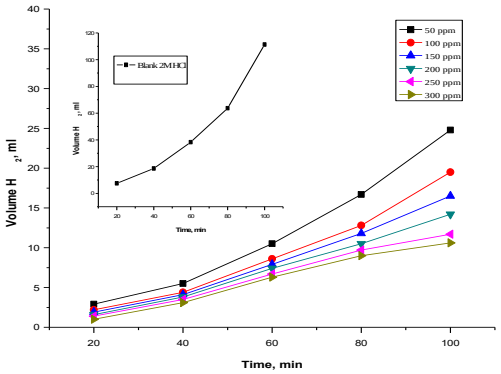


**Figure 1.** Amounts of emitted $H_2$ gas vs. time for dissolution of Al in 2 M HCl with and without several concentrations of CIE at 25ºC.

### 3.2. Mass loss Calculations.

The mass losses of Al in 2 M HCl without and in the nearness of different doses (50-300 ppm) of CIEwere resolved. Figure 2 illustrates the time mass loss micrographs without and with of changed concentrations of inhibitor at 25 °. The mass loss diminishes with expanding CIE concentration. The obtained information about the values of % IE, dissolution rate (CR) and the surface coverage (θ) for Al in 2M HCl and within various concentrations of CIEat several temperatures are appeared in Table 3.

*2.2.3.3. X-Ray photoelectron spectroscopy (XPS) analysis.*

The examination of (XPS) is a quantitative procedure for measuring the elemental composition of the surface of a material and indicated the binding energies of all presented elements.

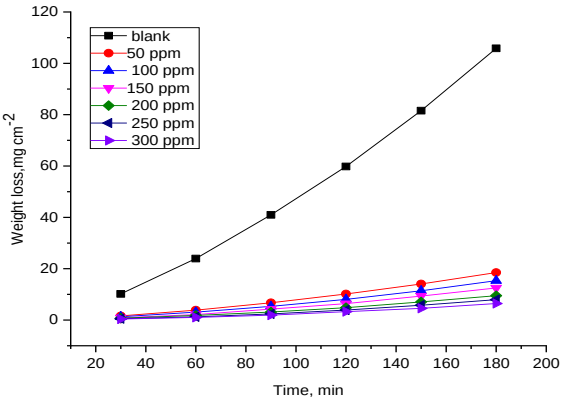


**Figure 2.** Mass loss-time curves for the dissolution of Al in 2M HCl without and with different amounts of CIEat 25°C

**Table 3.** Dissolution rate (C.R.) and inhibition efficiency outcomes resulted from mass loss technique for Al in 2 M HCL mediums at several amounts of CIE at 25°C.

| Conc., ppm | C.R., $mg.cm^{-2}.min^{-1}$ | θ | %IE |
|---|---|---|---|
| **blank** | 0.455 | …… | …… |
| **50** | 0.075 | 0.835 | 83.5 |
| **100** | 0.059 | 0.869 | 86.9 |
| **150** | 0.048 | 0.896 | 89.6 |
| **200** | 0.035 | 0.924 | 92.4 |
| **250** | 0.026 | 0.942 | 94.2 |
| **300** | 0.021 | 0.953 | 95.3 |

#### *3.2.1. Adsorption techniques.*

To comprehend the system of dissolution inhibiting impact, the adsorption attitude of the CIE adsorbents on the outer surface should be studied. The adsorption process is dependent on some variables, for example, the synthesis of the inhibitor, chemical composition and the properties of the ionized metal. There are various numerical expressions having along these lines formed to mull over of non-perfect effects. The most utilized isotherms are Frumkin, De Boer, Langmuir, Temkin, Flory-Huggins and Bockris-Swinkless [30-34]. The assessments of (θ) comparing to various amounts of CIE at 25-45 $^{0}$C have been utilized to select the best isotherm process. The adsorption of CIE molecules obeys the Langmuir adsorption [35] discussed as:

$$\left(\frac{\theta}{1-\theta}\right) = K_{ads}\ C \quad (7)$$

Where C is the concentration of CIE in the tested solutions, θ is the grade of surface coverage, $K_{ads}$ is the adsorption parameter. Straight lines are resulted from graphing of θ / (1-θ) against C with slope identical to $K_{ads}$ as showed up in Figure 3. All adsorption calculations were resolved. The obtained parameters are the free energy ($\Delta G^{\circ}_{ads}$), the heat of enthalpy ($\Delta H^{\circ}_{ads}$) and the entropy ($\Delta S^{\circ}_{ads}$). These amounts can be dictated by several systems relying on the estimations of $K_{ads}$ at various temperatures [36]. The $\Delta G^{\circ}_{ads}$ can be resolved from eq. (8):

$$K_{ads} = (1/55.5) \exp(-\Delta G^{\circ}_{ads} / RT) \quad (8)$$

Where 55.5 is the concentration of $H_2O$ in mol $l^{-1}$, R is the universal gas constant, and T is the temperature. ($\Delta H^\circ_{ads}$), ($\Delta S^\circ_{ads}$) can be calculated from eqs. (9 &10):

$$\text{Log } K_{ads} = (\Delta H^\circ_{ads} / 2.303RT) + \text{constant} \quad (9)$$

$$\Delta G^\circ_{ads} = \Delta H^\circ_{ads} - T\Delta S^\circ_{ads} \quad (10)$$

Table 4 illustrates all the determined calculations for the extract on Al surface, and outlined that, the sign of $\Delta G^\circ_{ads}$ was negative that demonstrates that the adsorption of this inhibitor is a continuous procedure. The estimations of $\Delta G^\circ_{ads}$ of 40 kJ $mol^{-1}$ and larger related to charging moving from the inhibitor molecules to metal outer surface (chemisorption); those of 20 kJ.$mol^{-1}$ and smaller suggests the electrostatic relationship among the inhibited surface and charged natural particles in the majority of the medium exhibit a physisorption [37, 38].

The indicated calculations of $\Delta G^\circ_{ads}$ are -20 kJ.$mol^{-1}$ and lower that attributed to the electrostatic interaction between the charged particles and the charged metal (physical adsorption). $\Delta G^\circ_{ads}$ values rise (turn into more positive) with a development in temperature that exhibits that the adsorption system is an exothermic technique. The negative indication of $\Delta H^\circ_{ads}$ shows that the adsorption technique of the inhibitor atoms is an exothermic method. An exothermic procedure is ascribed to either physisorption or chemisorption but endothermic technique is credited to chemisorption [39].

Enthalpy calculations up to 41.9 kJ.$mol^{-1}$ are ascribed to physisorption but those equal to100 kJ.$mol^{-1}$ and larger are related to chemisorption. The obtained estimations of $\Delta H^\circ_{ads}$ of CIEin 2M HCl are negative exhibiting that CIE may be physisorbed. The $\Delta S^\circ_{ads}$ are negative which is identified with exothermic adsorption process and delineated that the inhibitor particles, moving freely in the electrolyte were adsorbed in an organized way onto the Al surface.

### 3.2.2. Temperature influence and activation factors of inhibition procedure.

The impact of temperature on the dissolution average of Al in 2 M HCl without and in the nearness of the examined extract was shown in temperatures from 25 to 45 °C. The inhibitive ability diminishes with an expansion in temperature and the rate of dissolution rises. The decrease in the inhibition effectiveness with temperature is ascribed to the desorption of CIE particles from the examined surface. Plots of (log $k_{corr}$) with (1/T) for Al in 2 M HCl at various amounts of the extract are straight relations with slope $-E^*_a/2.303R$. These calculations acquired from the Arrhenius-type equation as followed:

$$k_{corr} = A \exp (E^*_a /RT) \quad (11)$$

Where $k_{corr}$ is the corrosion rate, $E^*_a$ is the activation energy, R is the universal gas constant, T is the temperature and A is the Arrhenius parameter. Estimations of $E^*_a$ of dissolution of Al in 2M HCl without and with several amounts of CIE were settled from the plotting of log ($k_{corr}$) against 1/T and are showed up in Figure 5 .The appointed meaning of transition state relationship is showed up in eq. (12):

$$K_{corr} = (RT/Nh) \exp (\Delta S^*/R) \exp (-\Delta H^*/RT) \quad (12)$$

Where h is Planck's steady, N is Avogadro's number, $\Delta S^*$ is the activated entropy and $\Delta H^*$ is the activated enthalpy. Figure 6 shows a graph of (log $k_{corr}$/T) versus (1/T). Straight relations are obtained with slopes proportional to ($\Delta H^*$/2.303R), their assessments are recorded in Table 5. The increase in $E^*a$ values in the existence of CIE than the corrosive solution indicates that the inhibitor is physisorbed on the Al metal surface [40]. Table 5 demonstrates that $E^*a$ rises with rising CIE amounts, recommending unexpected adsorption of the analyzed extract on the Al outer surface. The positive signs of $\Delta H^*$ indicated the endothermic thought of the Al dissolution procedure. The negative $\Delta S^*$ illustrates that in the rate predominant step, the association of unstable coordinated particles is higher than the dissociation [41, 42].

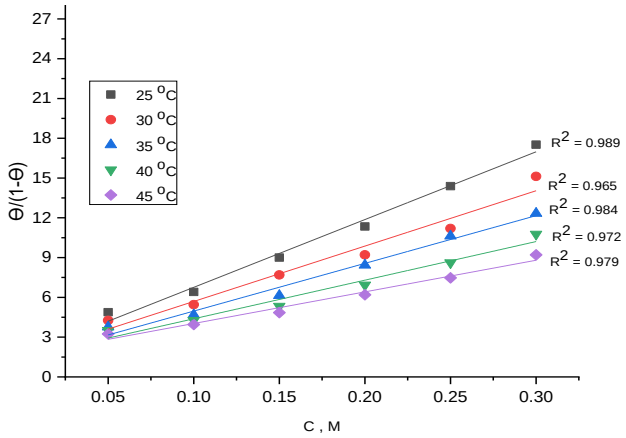


**Figure 3.** Curves of dissolution products for Al in 2M HCl in the existence of several amount of CIE to the Langmuir isotherm at various temperatures.

**Table 4.** Thermodynamic calculations for the adsorption of CIE on Al surface in 2M HCl at various temperatures.

| Temperature , C° | $G^\circ_{ads}$ , -Δ KJ $mole^{-1}$ | $-\Delta H^\circ_{ads}$ , kJ $mol^{-1}$ | $-\Delta S^\circ_{ads}$ , J $mol^{-1}K^{-1}$ |
|---|---|---|---|
| 25 | 19.7 | 29.7 | **33.6** |
| 30 | 19.5 | | **33.7** |
| 35 | 19.4 | | **33.4** |
| 40 | 19.2 | | **33.5** |
| 45 | 19.0 | | **33.6** |

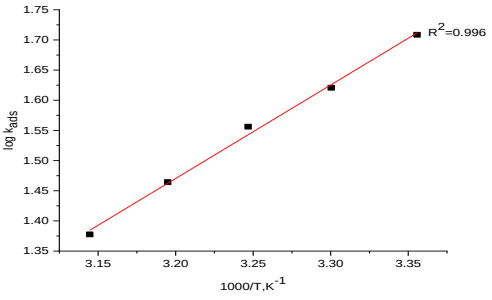


**Figure 4.** (Log $K_{ads}$) against (1/T) for the dissolution of Al in 2M HCl in the existence of Cichorium Intybus extract.

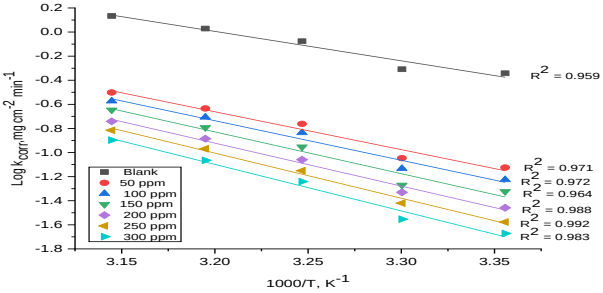

**Figure 5.** Arrhenius graphs for Al dissolution rates ($k_{corr.}$) after 90 minute of dipping in 2M HCl in the absence and existence of several amounts of Cichorium Intybus extract.

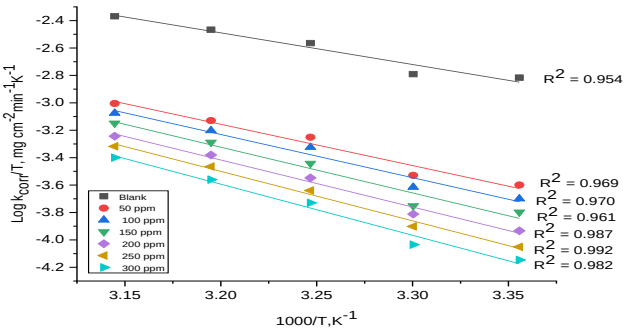


**Figure 6.** Transition-state for Al corrosion rates ($k_{corr}$) in 2M HCl in the non-existence and existence of varied concentrations of Cichorium Intybus extract.

**Table 5.** Activation calculations for Al dissolution in the non-existence and existence of varied concentrations of CIEin 2M HCl.

| Concentrations, ppm | Activation calculations | | |
|---|---|---|---|
| | $E^*_a$, kJ mol$^{-1}$ | $\Delta H^*$, kJ mol$^{-1}$ | $-\Delta S^*$, J mol$^{-1}$ K$^{-1}$ |
| Blank | 44.1 | 41.5 | **111.9** |
| 50 | 60.2 | 57.6 | **73.5** |
| 100 | 62.9 | 60.3 | **66.2** |
| 150 | 66.5 | 63.9 | **56.8** |
| 200 | 68.3 | 65.7 | **52.7** |
| 250 | 71.7 | 69.2 | **43.3** |
| 300 | 74.0 | 71.4 | **37.9** |

### 3.3. Electrochemical impedance spectroscopy method (EIS).

The dissolution action of Al in 2 M HCl medium with and without varying amounts of CIE was explained by the EIS strategy at 25 ± 1° C during 30 min of submersion. Figure (7) illustrates the Nyquist graph for Al in 2M HCl solution of action in the non-attendance and attendance of changed amounts of the analyzed extract. The way that EIS graphs have an around semi-round occurrence demonstrates that the dissolution of Al in 2 M HCl is compelled by a charge transfer resistance procedure. A little bending was found in specific frameworks, and the deformation has been credited to repeat dissipating [43] on account of surface obnoxiousness, defilements, divisions, grain limits, plan of penetrable layers, and Heterogeneity of the exposed surface. The width of the capacitive circle rises with the extension of concentration and decisive of the grade of inhibitive mechanism.

Despite the elevated frequency capacitive loop, the semi-loops turned and stretched up to the fourth quadrant, and an artificial-inductive loop at a smaller frequency limit was watched, demonstrating that the faradic technique is happening on the terminal areas. The inductive circle is all around credited to the adsorption of kinds coming about on account of the Al dissolution and the $H_2$ adsorption [44]. The equivalent circuit showed up in Figure 8 was utilized to fit impedance results. the acquired impedance results. This loop contains the solution resistance ($R_s$), the charge transfer resistance ($R_{ct}$), the inductance (L), the inductive resistance ($R_L$), and the capacitance of double layer ($C_{dl}$) [45]. A great fit with EIS was observed from our test information. Exactly when an inductive circle is accessible, the resistance of polarization ($R_P$) is resolved from eq. (13):

$$R_P = (R_{ct} \times R_L) / (R_{ct} + R_L) \qquad (13)$$

EIS outcomes from Table 6 illustrates that the $R_P$ calculations rise and the $C_{dl}$ estimations diminish with the extension of CIEamounts. This is due to the consistent substitution of $H_2O$ by the adsorption of the CIE particles on the studied metal, and reducing the level of the dissolution process.

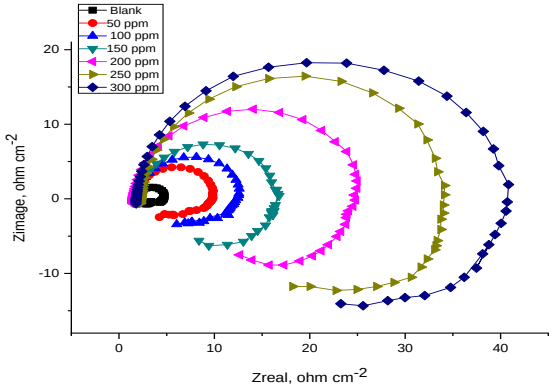


**Figure 7.** Nyquist graphs for Al in 2M HCl in the non-attendance and existence of different amounts of CIEat 25°C.

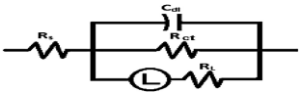


**Figure 8.** Electrical equivalent loop utilized to fit EIS measurements.

**Table 6.** Electrochemical calculations resulted from EIS method for Al in 2M HCl in the non-attendance and existence of different amounts of CIEat 25°C.

| Conc., ppm | $R_p$, Ω cm$^2$ | $C_{dl}$, μFcm$^{-2}$ | θ | %IE |
|---|---|---|---|---|
| **Blank** | 1.44 | 75.67 | ---- | ---- |
| **50** | 4.75 | 31.52 | 0.691 | 69.7 |
| **100** | 5.44 | 27.54 | 0.793 | 73.5 |
| **150** | 6.91 | 24.67 | 0.821 | 79.2 |
| **200** | 8.48 | 21.19 | 0.855 | 83.0 |
| **250** | 10.72 | 16.29 | 0.876 | 86.6 |
| **300** | 12.25 | 11.92 | 0.893 | 88.2 |

The bigger $R_P$ assessments are ascribed to a more inhibiting assembly [46, 47]. The decrease in the $C_{dl}$ is due to the increase of the dielectric constant or possibly from the increase of the thickness of the electrical double film, illustrating that the CIE particles inhibit the dissolution by adsorption at the metal/arrangement interface.

### 3.4. Tafel polarization method (TP).

Electrochemical procedures depend on current and potential estimations. It is commonly acknowledged that the inhibitor particles impede dissolution by adsorbing at the metal/medium interface. Tafel graphs of Al in 2 M HCl in the absence and nearness of changed amounts of CIEat 25°C are outlined in Figure 9. Polarization estimations were completed to give information about the potential of the cathodic and anodic responses. Different dissolution calculations, for example, corrosion current density ($i_{corr}$), corrosion potential ($E_{corr}$), Tafel slopes ($\beta_a$, $\beta_c$), the surface coverage area (θ) and the inhibition efficiency (%IE) are listed in Table 7. It is observed that the obtained results that the increase of the extract doses cause a huge reduction in cathodic and anodic flows. It might be reasoned that this extract appears as an inhibitor of mixed type, implying that the presence of CIE to 2M HCl solution decreases both the anodic corrosion of Al and impedes the cathodic $H_2$ development reaction.

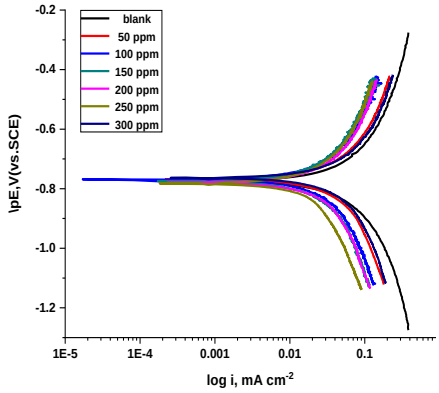


**Figure 9.** Tafel curves for the dissolution of Al in 2M HCl in the absence and presence of varied amounts of CIEat 25ºC

### 3.5. Electrochemical frequency modulation technique (EFM).

EFM is a nondestructive dissolution estimation system that can straightforwardly provide estimations of the dissolution current without earlier information on Tafel slopes. It is commonly acknowledged that the dissolution estimations decided from EFM procedure have accurate qualities than those obtained from different methods showing low dissolution values [48]. The modulation frequencies that are utilized in EFM procedure are in the capacitive district of the impedance spectrum. Calculations of the EFM system demonstrated a great understanding of dissolution rates got with the Tafel induction technique. Figure 10 is case of aluminum dipped in 2 M HCl mediums and in nearness of varied concentrations of CIE at 25°C. Table 8 demonstrates the determined dissolution calculations at various amounts of the examined inhibitor in 2 M HCl at 25°C (icorr, βa, βc, CF-2, CF-3 and % IE). From Table 8, the corrosion current densities decline by increasing the presence of CIE and the effectiveness of inhibition rises by expanding examined inhibitor concentration. The causality factors are near theoretical qualities, which as indicated by EFM theory [49] should ensure the validity of Tafel slopes and dissolution current densities. Estimations of causality factors show that the deliberate information is of acceptable quality. The known qualities for CF-2 and CF-3 are 2.0and 3.0, individually. The variation of causality parameters from their optimal qualities may be because of the disruption amplitude which was excessively little or which the goals of the frequency range aren't sufficiently high. The outcomes demonstrated a great understanding of dissolution parameters got with the EFM, TP and EIS techniques.

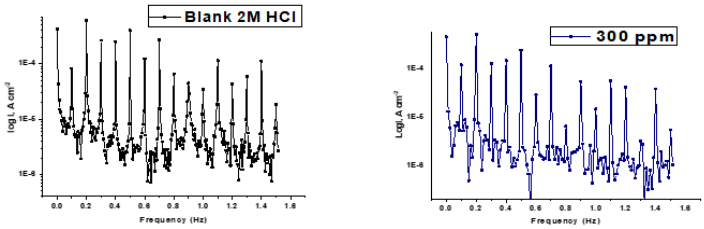


**Figure 10.** EFM spectra for Al in 2M HCl without and with existence of 300 ppm of CIE at 25ºC.

### 3.6. Atomic force microscopy (AFM) analysis.

AFM is a significant test for estimating the roughness of the examined surface at a most extreme resolution in fraction of nanometer [50]. AFM estimations can give accurate indications about the surface morphology of aluminum that is advantageous to dissolution process. The 3D of AFM pictures show up as appeared in Figure 11.

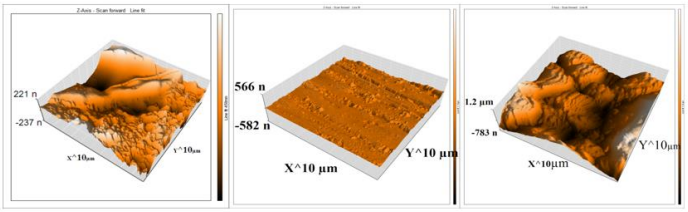


**Figure 11.** 3D AFM photographs of the surface of: A) cleaned Al surface; B) Al dipped in 2M HCl; C) Al dipped in 2M HCl having CIE(300 ppm).

The examined surface in 2M HCl has a higher coarseness (381.1 nm) than the cleaned Al outer surface (15.6 nm), that demonstrates that the examined surface is genuinely corroded in the destructive medium. The calculated coarseness of inhibited Al is diminished and reach to (67.5 nm).The observed softness of is because of the arrangement of a compressed adsorbed formation on the surface and then impeding the dissolution of Al [51].

### 3.7. FTIR examination.

FTIR procedure utilized for distinguishing of the existed functional groups in organic particles on the aluminum surface from the range 4000 to 400 $cm^{-1}$. Figure 13 illustrates the IR range of the pure extract and demonstrates that the layer was based on the aluminum after dipping for 4 hrs. in 2M HCl utilizing the extract with the optimum dose (300 ppm). In the spectrum of the pure extract in Figure 12, the (OH) frequency is at 3331$cm^{-1}$, the stretching $SP_3$–C–H frequency at 2974 and 2838 $cm^{-1}$, the stretching – C=O frequency at 1669 $cm^{-1}$, the bending –C–N– frequency shows up at 1088 $cm^{-1}$. FTIR illustrated a resistance barrier for aluminum in 2 M HCl utilizing 300 ppm of the examined extract after immersion for 4hrs [52].

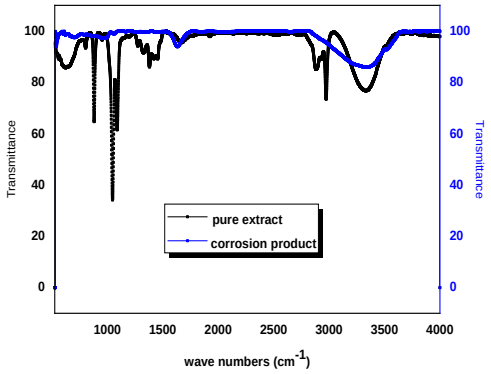


**Figure 12.** IR spectrum of pure extract and corrosion products of Aluminum after the weight loss test having 300 ppm of CIE at 25 °C.

The obtained outcomes demonstrated that there were little changes and some function group frequencies missed and others moved because of interference and coordination with $Al^{3+}$. In the inhibited solutions, the dissolution of aluminum was decreased by the formation of a defensive layer [53.54].

### 3.8. X-ray Photoelectron Spectroscopy (XPS).

XPS examination was applied to provide accurate details into the chemical nature of the interface among the examined inhibitor and the Al surface. The XPS spectrum of Al 2p, C1s, Cl 2p, N 1s, O 1s resulted for aluminum after submersion in 2M HCl

solution in the existence of 300 ppm of (CIE) for 24 hrs. Following deconvolution as appeared in Figure 13. The Al 2p spectrum illustrated one peak existed at a binding energy (BE) of 74.42 eV which corresponds to $Al_2O_3$ Figure 13a [55].

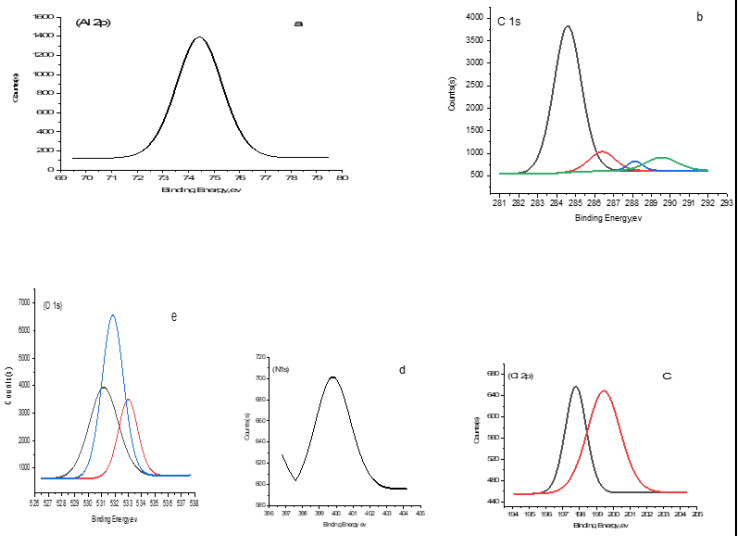


**Figure 13.** XPS curves of (a) Al 2p, (b) C 1s, (c) Cl 2p, (d) N 1s, (e) O 1s for Al in 2 M HCl.

The spectrum of C 1s Figure 13b is deconvoluted into four tops: the first one at 284.58 eV which is ascribed to (C–C) bond in aromatic rings, the next peak situated at 286.41 eV binding energy that is ascribed to the (C–O–C) aromatic bonds, The third peak at 288.14 which related to (C=O), The fourth peak located at 289.54 that corresponds to (–COO) [56]. The Cl 2p Figure 13c is deconvoluted into two tops existed at 197.7 eV for Cl 2p3/2 and 198.99 eV for Cl 2p1/2 [57]. The spectrum of N 1s appears as one peak located at 399.78 eV that attributed to N in aromatic rings as pyridine Figure 13d. The spectrum of O1s Figure 13e is deconvoluted into three peaks, The first peak at 531.28 can be attributed to $Al(OH)_3$, the second one at 531.88 eV that related to C–O bond, while the third top situated at 532.27 eV binding energy which identified with the C-O-C aromatic bonds. Finally, the XPS spectrum proved the existence of a defensive film of Cichorium Intybus extract.

### 3.9. Inhibitive mechanism.

CIE utilized as an inhibitor caused variation in the Tafel slopes, a decline the dissolution current density, an expansion in the polarization resistance ($R_p$) and decreasing in the capacitance of double layer ($C_{dl}$) through the obstruction in the dissolution reactions. The inhibitive mechanism is related to the physisorption process of Cichorium Intybus particles on the Al surface. The majority of the Cichorium Intybus constituents are chalcone, scopoletin, mandelic Acid, lupeol and naphthalene. These particles may impede the dissolution due to:

a. Chemical complexes formed through coordinating with $Al^{3+}$ cations that adsorbed on Al surface, in this manner preventing the adsorption aggressive particles, for example $Cl^-$ ions.

b. The adsorption of CIE particles on the Al surface because of the donnor acceptor interference among π electrons of donor atoms of organic rings of the particles and the vacant d orbital of Al surface molecules

c. The particles in CIEcan likewise be adsorbed on Al outer surface as negatively charged molecules that can react electrostatically with positively charged metal surface, which prompted rising in %IE and the surface coverage area. CIEgives more IE because of the high level of surface coverage coming about because of the adsorption of specific particles from the pure Cichorium Intybus [58].

**Table 7.** Outcomes from tafel calculations of Al in 2M HCl having varied amounts of CIEat 25ºC

| Conc., ppm | -$E_{corr}$, mV | $i_{corr}$, mA $cm^{-2}$ | $\beta_a$ V $dec^{-1}$ | $\beta_c$ V $dec^{-1}$ | C.R , mpy | Θ | % IE |
|---|---|---|---|---|---|---|---|
| **0** | 774.0 | 847.0 | 7.648 | 5.23 | 363.9 | ---- | ---- |
| **50** | 752.3 | 175.6 | 3.78 | 3.91 | 71.3 | 0.793 | 79.3 |
| **100** | 802.1 | 142.1 | 3.41 | 3.82 | 60.6 | 0.832 | 83.2 |
| **150** | 811.3 | 110.5 | 3.09 | 3.67 | 48.8 | 0.870 | 87.0 |
| **200** | 765.1 | 87.9 | 2.89 | 3.51 | 35.7 | 0.896 | 89.6 |
| **250** | 711.2 | 60.3 | 2.65 | 3.31 | 30.5 | 0.929 | 92.9 |
| **300** | 789.5 | 45.5 | 2.37 | 2.92 | 27.1 | 0.946 | 94.6 |

**Table 8.** Electrochemical outcomes got from EFM for in the non-existence and existence of varied amounts of CIEat 25ºC

| Conc., ppm | $i_{corr}$ , µA$cm^{-2}$ | $\beta_a$, mV$dec^{-1}$ | $\beta_c$, mV$dec^{-1}$ | CF-2 | CF-3 | C.R , mpy | θ | %IE |
|---|---|---|---|---|---|---|---|---|
| **Blank** | 831.4 | 67.4 | 39.1 | 1.85 | 1.68 | 357.0 | ---- | ---- |
| **50** | 253.7 | 32.2 | 37.1 | 2.37 | 1.64 | 113.5 | 0.695 | 69.5 |
| **100** | 238.4 | 25.2 | 26.3 | 1.99 | 1.75 | 102.4 | 0.713 | 71.3 |
| **150** | 217.6 | 21.8 | 23.1 | 1.95 | 2.19 | 93.4 | 0.738 | 73.8 |
| **200** | 212.8 | 20.7 | 22.4 | 2.52 | 1.93 | 91.4 | 0.744 | 74.4 |
| **250** | 208.9 | 19.8 | 21.9 | 2.89 | 2.19 | 89.7 | 0.749 | 74.9 |
| **300** | 193.7 | 17.6 | 19.4 | 2.05 | 3.28 | 81.2 | 0.767 | 76.7 |

## 4. CONCLUSIONS

CIEhas been dissolution inhibitory influence on Al in 2 M HCl corrosive solution. There are acceptable calculations among chemical and electrochemical measurements. Polarization outcomes noticed that the CIEis an inhibitor of mixed-type. Dissolution protection efficiencies and the energy of corrosion activation rise with temperature elevation. The adsorption of CIEis

ascribed to the Langmuir isotherm (physisorption). AFM procedure provides data about morphology of the metal surface. FTIR examination of the extract and dissolution product demonstrated the functional groups that have coordinated with $Al^{+3}$. The XPS examination proved the development of a defensive film of CIE on Al surface.

## 5. REFERENCES


1. Fouda, A.S., El-Awady, G.Y. & El Behairy, W.T. Prosopis juliflora Plant Extract as Potential Corrosion Inhibitor for Low-Carbon Steel in 1 M HCl Solution. J Bio Tribo Corros 2018, 4, 8, https://doi.org/10.1007/s40735-017-0124-x.
2. Ouali, I.E.; Hammouti, B.; Aouniti, A.; Ramli, Y.; Azougagh, M.; Essassi, E.M.; Bouachrine, M.J. Inhibition of acid Corrosion of Aluminum using Salvadore persica. *Environmental Science* **2010,** *1*.
3. Ahmed, A.H.; Hassan, A.M.; Gumaa, H.A.; Mohamed, B.H.; Eraky, A.M. Mn2+-complexes of n,o-dihydrazone: structural studies, indirect band gap energy and corrosion inhibition on aluminum in acidic medium. *Journal of the Chilean Chemical Society* **2018**, *63*, 4180-4189, http://dx.doi.org/10.4067/S0717-97072018000404180.
4. El-Sherbini, A.E.E.F.; Khalil, B.M.M.H.; Ismail, C.E.H.; Tobar, D.S.S. The Corrosion of Copper Metal in HCl Solutions and the effect of Molybdate and Chromate. *International Conference on Aerospace Sciences and Aviation Technology* **2015**, *16*, 1-9, http://dx.doi.org/10.21608/ASAT.2015.22941.
5. Sanaei, Z.; Ramezanzadeh, M.; Bahlakeh, G.; Ramezanzadeh, B. Use of Rosa canina fruit extract as a green corrosion inhibitor for mild steel in 1M HCl solution: A complementary experimental, molecular dynamics and quantum mechanics investigation. *Journal of Industrial and Engineering Chemistry* **2019**, *69*, 18-31, https://doi.org/10.1016/j.jiec.2018.09.013.
6. Farahati, R.; Mousavi-Khoshdel, S.M.; Ghaffarinejad, A.; Behzadi, H. Experimental and computational study of penicillamine drug and cysteine as water-soluble green corrosion inhibitors of mild steel. *Progress in Organic Coatings* **2020**, *142*, https://doi.org/10.1016/j.porgcoat.2020.105567.
7. Raghavendra, N.; Hublikar, L.V.; Patil, S.M.; Ganiger, P.J.; Bhinge, A.S. Efficiency of sapota leaf extract against aluminium corrosion in a 3 M sodium hydroxide hostile fluid atmosphere: a green and sustainable approach. *Bulletin of Materials Science* **2019**, *42*, 226, https://doi.org/10.1007/s12034-019-1922-1.
8. Kokalj, A.; Peljhan, S.; Finšgar, M.; Milošev, I. What Determines the Inhibition Effectiveness of ATA, BTAH, and BTAOH Corrosion Inhibitors on Copper? *Journal of the American Chemical Society* **2010**, *132*, 16657-16668, https://doi.org/10.1021/ja107704y.
9. Noor, E.A.; Al-Moubaraki, A.H.; Al-Ghamdi, A.A. Continuous Studies on Using Camel's Urine as Nontoxic Corrosion Inhibitor–Corrosion Inhibition of Al–Cu Alloy in Alkaline Solutions. *Arabian Journal for Science and Engineering* **2019**, *44*, 237-250, https://doi.org/10.1007/s13369-018-3489-3.
10. Chaubey, N.; Singh, V.K.; Quraishi, M.A. Electrochemical approach of Kalmegh leaf extract on the corrosion behavior of aluminium alloy in alkaline solution. *International Journal of Industrial Chemistry* **2017**, *8*, 75-82, https://doi.org/10.1007/s40090-016-0103-y.
11. Yazdzad, A.R.; Shahrabi, T.; Hosseini, M.G. Inhibition of 3003 aluminum alloy corrosion by propargyl alcohol and tartrate ion and their synergistic effects in 0.5% NaCl solution. *Materials Chemistry and Physics* **2008**, *109*, 199-205, https://doi.org/10.1016/j.matchemphys.2007.11.012.
12. Aejitha, S.; Kasthuri, P.K.; Jyothi, S. Corrosion inhibitory action of Commiphora caudata extract on the mild steel corrosion in 1 M H2SO4 acid medium. *Journal of Adhesion Science and Technology* **2016**, *30*, 784-802, https://doi.org/10.1080/01694243.2015.1118284.
13. Fouda, A.S.; Megahed, H.E.; Fouad, N.; Elbahrawi, N.M. Corrosion Inhibition of Carbon Steel in 1 M Hydrochloric Acid Solution by Aqueous Extract of Thevetia peruviana. *Journal of Bio- and Tribo-Corrosion* **2016**, *2*, 1-16, https://doi.org/10.1007/s40735-016-0046-z.
14. de Souza, F.S.; Giacomelli, C.; Gonçalves, R.S.; Spinelli, A. Adsorption behavior of caffeine as a green corrosion inhibitor for copper. *Materials Science and Engineering: C* **2012**, *32*, 2436-2444, https://doi.org/10.1016/j.msec.2012.07.019.
15. Nazeer, A.A.; Shalabi, K.; Fouda, A.S. Corrosion inhibition of carbon steel by Roselle extract in hydrochloric acid solution: electrochemical and surface study. *Research on Chemical Intermediates* **2015**, *41*, 4833-4850, https://doi.org/10.1007/s11164-014-1570-4.
16. Khadraoui, A.; Khelifa, A.; Hachama, K.; Mehdaoui, R. Thymus algeriensis extract as a new eco-friendly corrosion inhibitor for 2024 aluminium alloy in 1M HCl medium. *Journal of Molecular Liquids* **2016**, *214*, 293-297, https://doi.org/10.1016/j.molliq.2015.12.064.
17. Abdallah, Y.M.; Hassan, H.M.; Shalabi, K.; Fouda, A.S. Effects of arctostaphylos uva-ursi extract as green corrosion inhibitor forCu10Ni Alloy in 1 M HNO3. *Int J. Electrochem Sci* **2014,** *9*, 5073-5091.
18. Shalabi, K.; Fouda, A.S.; Elewady, G.Y.; El-Askalany, A. Adsorption and inhibitive properties of Phoenix dactylifera L. Extract as a green inhibitor for aluminum and aluminum-silicon alloy in HCl. *Protection of Metals and Physical Chemistry of Surfaces* **2014**, *50*, 420-431, https://doi.org/10.1134/S2070205114030174.
19. Fouda, A.; Abdallah, Y.; Elawady, G.Y.; Ahmed, R.M. Electrochemical study on the effectively of Hyoscyamus Muticus Extract as a green inhibitor for corrosion of copper in 1 MHNO3. *Journal of Materials and Environmental Science* **2015**, *6*, 1519-1531.
20. Saied, S.; Shah, S.; Ali, Z.; Khan, A.; Marasini, B.P.; Choudhary, M.I. Chemical Constituents of Cichorium intybus and their Inhibitory Effects against Urease and α-Chymotrypsin Enzymes. *Natural Product Communications* **2011**, *6*, 17-22, https://doi.org/10.1177/1934578X1100600817.
21. Nwafor, I.C.; Shale, K.; Achilonu, M.C. Chemical Composition and Nutritive Benefits of Chicory *(Cichorium intybus*) as an Ideal Complementary and/or Alternative Livestock Feed Supplement. *The Scientific World Journal* **2017**, *2017*, 11, https://doi.org/10.1155/2017/7343928.
22. Obot, I.B.; Ankah, N.K.; Sorour, A.A.; Gasem, Z.M.; Haruna, K. 8-Hydroxyquinoline as an alternative green and sustainable acidizing oilfield corrosion inhibitor. *Sustainable Materials and Technologies* **2017**, *14*, 1-10, https://doi.org/10.1016/j.susmat.2017.09.001.
23. Khaled, K.F. Guanidine derivative as a new corrosion inhibitor for copper in 3% NaCl solution. *Materials Chemistry and Physics* **2008**, *112*, 104-111, https://doi.org/10.1016/j.matchemphys.2008.05.052.
24. Abdel-Rehim, S.S.; Khaled, K.F.; Abd-Elshafi, N.S. Electrochemical frequency modulation as a new technique for monitoring corrosion inhibition of iron in acid media by new thiourea derivative. *Electrochimica Acta* **2006**, *51*, 3269-3277, https://doi.org/10.1016/j.electacta.2005.09.018.
25. Al-Mobarak, N.A.; Khaled, K.F.; Hamed, M.N.H.; Abdel-Azim, K.M.; Abdelshafi, N.S. Corrosion inhibition of copper in chloride media by 2-mercapto-4-(p-methoxyphenyl)-6-oxo-1,6-

dihydropyrimidine-5-carbonitrile: Electrochemical and theoretical study. *Arabian Journal of Chemistry* **2010**, *3*, 233-242, https://doi.org/10.1016/j.arabjc.2010.06.007.
26. Khaled, K.F. Evaluation of electrochemical frequency modulation as a new technique for monitoring corrosion and corrosion inhibition of carbon steel in perchloric acid using hydrazine carbodithioic acid derivatives. *Journal of Applied Electrochemistry* **2009**, *39*, 429-438, https://doi.org/10.1007/s10800-008-9688-y.
27. Khaled, K.F. Application of electrochemical frequency modulation for monitoring corrosion and corrosion inhibition of iron by some indole derivatives in molar hydrochloric acid. *Materials Chemistry and Physics* **2008**, *112*, 290-300, https://doi.org/10.1016/j.matchemphys.2008.05.056.
28. Shalabi, K.; Abdallah, Y.M.; Fouda, A.S. Corrosion inhibition of aluminum in 0.5 M HCl solutions containing phenyl sulfonylacetophenoneazo derivatives. *Research on Chemical Intermediates* **2015**, *41*, 4687-4711, https://doi.org/10.1007/s11164-014-1561-5.
29. Hsissou, R.; Benzidia, B.; Rehioui, M.; Berradi, M.; Berisha, A.; Assouag, M.; Hajjaji, N.; Elharfi, A. Anticorrosive property of hexafunctional epoxy polymer HGTMDAE for E24 carbon steel corrosion in 1.0 M HCl: gravimetric, electrochemical, surface morphology and molecular dynamic simulations. *Polymer Bulletin* **2019**, https://doi.org/10.1007/s00289-019-02934-5.
30. Motawea, M.M.; Gadow, H.S.; Fouda, A.S. Expired Cidamex Drug as Corrosion Inhibitor for Aluminum in Acidic Solution. *Researches in Engineering* **2016,** *16*, 1-16.
31. Zaroual, A.; El Qouatli, S.; Bellouchou, A.; Guenbour, A.; Najih, R.; Chtaini. A. An Electrochemical Sensor for the Detection of p-Anisidine through Electrochemistry. *The Global Journal of Researches in Engineering* **2016**, *16*, 1-10.
32. Roy, P.; Saha, S.K.; Banerjee, P.; Dey, S.; Sukul, D. Experimental and theoretical investigation towards anti-corrosive property of glutamic acid and poly-γ-glutamic acid for mild steel in 1 M HCl: intramolecular synergism due to copolymerization. *Research on Chemical Intermediates* **2017**, *43*, 4423-4444, https://doi.org/10.1007/s11164-017-2887-6.
33. Amin, A.; Khaled, K.F.; Mohsen, Q.; Arida, A.H. New Cyanoacetamide Derivatives as Corrosion Inhibitors for Carbon Steel in Acidic Media. *Corrosion Science* **2010**, *52*, 1684.
34. Umoren, A.A.; Ogbobe, O.; Igwe, I.O.; Ebenso, E.E. Use of Rosmarinus officinalis as Green Corrosion Inhibitor for Carbon Steel in Acid Medium. *Corrosion Science* **2008,** *50*, 1998, https://doi.org/10.4236/ajac.2014.52009. 35. Hassan, M.R.; Zaafarany, A.I. Kinetics of Corrosion Inhibition of Aluminum in Acidic Media by Water-Soluble Natural Polymeric Pectates as Anionic Polyelectrolyte Inhibitors. *Materials* **2013**, *6*, 2436-2451, https://doi.org/10.3390/ma6062436.
36. Fouda, A.S.; Mohamed, F.S.; El-Sherbeni, M.W. Corrosion Inhibition of Aluminum–Silicon Alloy in Hydrochloric Acid Solutions Using Carbamidic Thioanhydride Derivatives. *Journal of Bio- and Tribo-Corrosion* **2016**, *2*, 11, https://doi.org/10.1007/s40735-016-0039-y.
37. Haruna, K.; Obot, I.B.; Ankah, N.K.; Sorour, A.A.; Saleh, T.A. Gelatin: A green corrosion inhibitor for carbon steel in oil well acidizing environment. *Journal of Molecular Liquids* **2018**, *264*, 515-525, https://doi.org/10.1016/j.molliq.2018.05.058.
38. Abd El Rehim, S.S.; Sayyah, S.M.; El-Deeb, M.M.; Kamal, S.M.; Azooz, R.E. Adsorption and corrosion inhibitive properties of P(2-aminobenzothiazole) on mild steel in hydrochloric acid media. *International Journal of Industrial Chemistry* **2016**, *7*, 39-52, https://doi.org/10.1007/s40090-015-0065-5.
39. Baran, E.; Cakir, A.; Yazici, B. Inhibitory effect of Gentiana olivieri extracts on the corrosion of mild steel in 0.5M HCl: Electrochemical and phytochemical evaluation. *Arabian Journal of Chemistry* **2019**, *12*, 4303-4319, https://doi.org/10.1016/j.arabjc.2016.06.008.
40. Verma, C.; Ebenso, E.E.; Bahadur, I.; Quraishi, M.A. An overview on plant extracts as environmental sustainable and green corrosion inhibitors for metals and alloys in aggressive corrosive media. *Journal of Molecular Liquids* **2018**, *266*, 577-590, https://doi.org/10.1016/j.molliq.2018.06.110.
41. Fouda, A.; Mohamed, A.E.; Khalid, M.A. Trigonella stellate extract as corrosion inhibitor for copper in 1M nitric acid solution. **2016**, *8*, 86-98.
42. Fouda, A.S.; Killa, H.M.; Farouk, A.; Salem, A.M. CalicotomeExtract as a Friendly Corrosion Inhibitor forCarbon Steel in Polluted NaClSolution: Chemical and Electrochemical Studies. *Egyptian Journal of Chemistry* **2019**, *62*, 1879-1894, https://doi.org/10.21608/EJCHEM.2019.7656.1649.
43. Fouda, A.S.; Abousalem, A.S.; El-Ewady, G.Y. Mitigation of corrosion of carbon steel in acidic solutions using an aqueous extract of Tilia cordata as green corrosion inhibitor. *International Journal of Industrial Chemistry* **2017**, *8*, 61-73, https://doi.org/10.1007/s40090-016-0102-z.
44. Jeeva, M.; Venkatesa Prabhu, G.; Rajesh, C.M. Inhibition effect of nicotinamide and its Mannich base derivatives on mild steel corrosion in HCl. *Journal of Materials Science* **2017**, *52*, 12861-12888, https://doi.org/10.1007/s10853-017-1401-2.
45. Ahmed, S.K.; Ali, W.B.; Khadom, A.A. Synthesis and investigations of heterocyclic compounds as corrosion inhibitors for mild steel in hydrochloric acid. *International Journal of Industrial Chemistry* **2019**, *10*, 159-173, https://doi.org/10.1007/s40090-019-0181-8.
46. El-Aziz, A.; Fouda, S.; Rabab, M.; Shahba, A.; El-Shenawy, A.E.; Taghreed, J.A.; Seyam, Evaluation of Cleome Droserifolia (Samwah) as Green Corrosion Inhibitor for Mild Steel in 1 M HCl Solution. *Int. J. Electrochem. Sci*. **2018,** *13*, 7057-7075, https://doi.org/10.20964/2018.03.54.
47. Fouda, A.S.; Ismail, M.A.; El-ewady, G.Y.; Abousalem, A.S. Evaluation of 4-amidinophenyl-2,2′-bithiophene and its aza-analogue as novel corrosion inhibitors for CS in acidic media: Experimental and theoretical study. *Journal of Molecular Liquids* **2017**, *240*, 372-388, https://doi.org/10.1016/j.molliq.2017.05.089.
48. Nathiya, R.S.; Perumal, S.; Moorthy, M.; Murugesan, V.; Rangappan, R.; Raj, V. Synthesis, Characterization and Inhibition Performance of Schiff Bases for Aluminium Corrosion in 1 M H2SO4 Solution. *Journal of Bio- and Tribo-Corrosion* **2019**, *6*, 5 https://doi.org/10.1007/s40735-019-0291-z.
49. Fouda, A.S.; El-Dossoki, F.I.; Shady, I.A. Adsorption and corrosion inhibition behavior of polyethylene glycol on α-brass alloy in nitric acid solution. *Green Chemistry Letters and Reviews* **2018**, *11*, 67-77, https://doi.org/10.1080/17518253.2018.14385.
50. Wang, B.; Zhang, L.; Su, Y.; Xiao, Y.; Liu, J. Corrosion behavior of 5A05 aluminum alloy in NaCl solution. *Acta Metallurgica Sinica (English Letters)* **2013**, *26*, 581-587,, https://doi.org/10.1007/s40195-013-0018-y.
51. Devi, P.N.; Sathiyabama, J.; Rajendran, S. Study of surface morphology and inhibition efficiency of mild steel in simulated concrete pore solution by lactic acid-Zn2+ system. *International Journal of Corrosion and Scale Inhibition* **2017**, *6*, 18-31, https://doi.org/10.17675/2305-6894-2017-6-1-2.
52. Fouda, A.S.; Abdel Aal, A.; Abdel Haleem, E. Calotropis procera extract (cpe) as corrosion inhibitor for copper in nitric acidic medium. *Bulletin of Faculty of Science, Zagazig University* **2017**, *2017*, 204-228, https://doi.org/10.21608/BFSZU.2017.31051.
53. Al-Nami, S. Calotropis Procera Extract as Corrosion Inhibitor for Copper in Nitric Acidic Environment. *International Journal of Electrochemical Science* **2019**, *14*, 6902-6919, https://doi.org/10.20964/2019.07.118.

54. Fouda, A.S.; Zaki, E.G.; Khalifa, M.M.A. Some New Nonionic Surfactants Based on Propane Tricarboxylic Acid as Corrosion Inhibitors for Low Carbon Steel in Hydrochloric Acid Solutions. *Journal of Bio- and Tribo-Corrosion* **2019**, *5*, 31, https://doi.org/10.1007/s40735-019-0223-y.
55. Le, T.T.T.; Le, N.; Pallavolu, M.R.; Jeon, Y.; Jeong, D.S.; Pejjai, B.; Reddy, V.R.M.; Truong, N.T.N.; Park, C. Green and low-cost preparation of CIGSe thin film by a nanocrystals ink based spin-coating method. *Korean Journal of Chemical Engineering* **2019**, *36*, 2110-2117, https://doi.org/10.1007/s11814-019-0386-8.
56. Halim, J.; Cook, K.M.; Naguib, M.; Eklund, P.; Gogotsi, Y.; Rosen, J.; Barsoum, M.W. X-ray photoelectron spectroscopy of select multi-layered transition metal carbides (MXenes). *Applied Surface Science* **2016**, *362*, 406-417, https://doi.org/10.1016/j.apsusc.2015.11.089.
57. Park, J.C.; Hwang, S.; Kim, J.M.; Kim, J.K.; Seo, J.H.; Choi, D.K.; Lee, H.S.; Cho, H. Low damage and anisotropic dry etching of high-k Dielectric HfO2 Films in Inductively Coupled Plasmas. *Electronic Materials Letters* **2010**, *6*, 107-112, https://doi.org/10.3365/eml.2010.09.107.
58. Fouda, A.S.; Megahed, H.E.; Fouad, N.; Elbahrawi, N.M. Corrosion Inhibition of Carbon Steel in 1 M Hydrochloric Acid Solution by Aqueous Extract of Thevetia peruviana. *Journal of Bio-and Tribo-Corrosion* **2016**, *2*, https://doi.org/10.1007/s40735-016-0046-z.

## 6. ACKNOWLEDGEMENTS

All our gratitude to the anonymous referees for their careful reading of the manuscript and valuable comments which helped in shaping this paper to the present form. We thank all laboratory staff of corrosion chemistry from the University of Mansoura (Egypt) for their kind cooperation.